



Dual-Polarization Tornadic Debris Signatures Part I: Examples and Utility in an Operational Setting

CHRISTOPHER J. SCHULTZ^{1,2}, LAWRENCE D. CAREY¹, ELISE V. SCHULTZ¹,
BRIAN C. CARCIONE³, CHRISTOPHER B. DARDEN³, CHRISTINA C. CROWE³,
PATRICK N. GATLIN^{2,4}, DAVID J. NADLER³, WALTER A. PETERSEN⁵, KEVIN R.
KNUPP¹

¹Department of Atmospheric Science, University of Alabama Huntsville, Huntsville, Alabama

²NASA Marshall Space Flight Center, Huntsville, Alabama

³National Weather Service, Huntsville, Alabama

⁴Earth System Science Center, University of Alabama Huntsville, Huntsville, Alabama

⁵NASA Wallops Flight Facility, Wallops, Virginia

(Manuscript received 2 March 2012; in final form 20 November 2012)

ABSTRACT

Dual-polarization examples of tornadic debris signatures (DPTDS) are presented from multiple tornadic events. Examples are from a variety of convective modes and at various ranges from the radar. The dual-polarization variable most useful in the detection of tornadic debris is correlation coefficient (ρ_{hv}), as this variable determines the homogeneity/heterogeneity of the scatterers found within a radar volume. In general, ρ_{hv} values below 0.70 that are collocated with a rotation signature indicative of a tornado and strong returned signal (horizontal radar reflectivity factor > 30 dBZ) are associated with debris from tornadoes. These signatures are associated with tornadoes rated EF-0 to EF-5 and in some cases could be seen out to ranges beyond 100 km. Also, DPTDS diameter and height are loosely tied to tornado strength, as higher rated tornadoes tended to have larger DPTDS diameters and loft debris to higher levels in the atmosphere. However, definitive relationships between EF-rating and radar signatures are not currently possible because of unknown and variable surface features (i.e., exactly what was damaged, when it was damaged, the degree to which things were damaged, etc.), lofted debris characteristics (e.g., shape, size, orientation, dielectric), and limits on available damage indicators during storm surveys. Part II of this study examines caveats of the dual-polarization signature, including data quality, signature to ground track location difference, scanning strategy limitations, and an event where DPTDS criteria were met using multiple proposed DPTDS criteria, but damage was not observed.

Corresponding author address: Christopher J. Schultz, NASA Marshall Space Flight Center, 320 Sparkman Dr., Huntsville, AL, 35805

E-mail: christopher.j.schultz@nasa.gov

1. Introduction

As polarimetric observations become more abundant as advances in radar technology are installed on the national scale, it will be important for meteorologists, emergency managers, and first responders to utilize new information to enhance severe and hazardous weather warnings or provide accurate and timely responses to various meteorological events. One such use will be detection of tornadoes as they are producing damage.

Previous work using single-polarization radar examined the detection of tornadic debris by using a combination of radar reflectivity factor at horizontal polarization and velocity (e.g., Bunkers and Baxter 2011, Forbes 2011). Thus, the observance of high horizontal radar reflectivity factor (Z_{HH}) values near tornadic circulations has been denoted as a “probable debris signature”, as one was not always confident that what is observed on radar is debris. This is especially true, for instance, if the tornado was surrounded by rain and hail. In Figure 1, Z_{HH} from the Weather Surveillance-88D radar located at Hytop, AL (Crum and Alberty 1993; KHTX) suggested that there might be a large probable debris signature on the southwest flank of the storm. This signature has also been described as a “debris ball” (e.g., Bunkers and Baxter 2011, Forbes 2011). However, dual-polarization information from the Advanced Radar for Meteorological and Operational Research (ARMOR, Petersen et al. 2007), shows that the lowering in correlation coefficient that is associated with tornadic debris (Fig. 1; bottom panel, dark blue region within white circle) is small, and much of the ball-like

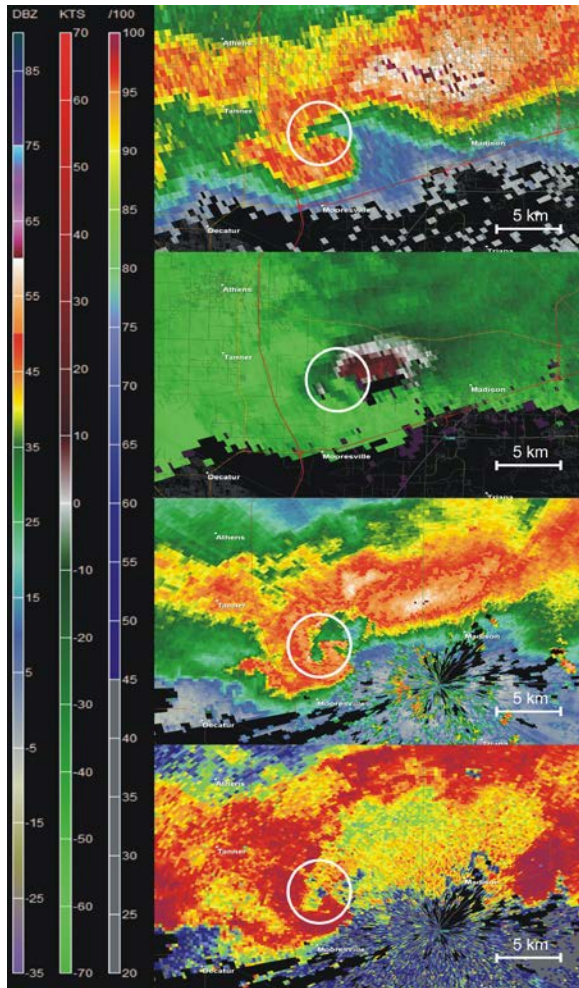


Figure 1. Presented is a plan position indicator (PPI) image from the WSR-88D located at Hytop, AL (KHTX; top two panels), and UAHuntsville’s ARMOR radar (bottom two panels) located at the Huntsville International Airport. The top two panels are Z_{HH} and V_r from KHTX at 2157 UTC on April 27, 2011, while the bottom two panels are Z_{HH} and ρ_{hv} from ARMOR at 2157 UTC on April 27, 2011. Scales on the left are as follows: reflectivity (dBZ), V_r (KTS), and ρ_{hv} (value*100.0). White circles denote the tornadic circulation. The dark blue region within the white circle in the bottom panel is where the tornadic debris is identified.

appearance in the WSR-88D Z_{HH} was due to rain and small hail wrapping around the back side of the tornado.

There are also times when hail can be located in a region where a tornado might be present and can mimic debris ball signatures that have been observed in the past with large tornadoes. A tornado warned supercell from March 26, 2011, provides such an example (Fig. 2). This storm has strong reflectivity (>65 dBZ) in its southwest flank and even an appearance of a wake signature in Z_{HH} that has

been seen in Great Plains tornadic supercells (e.g., Ryzhkov et al. 2005, Van Den Broeke et al. 2008). No tornado was ever confirmed with this storm; however, local media misidentified this reflectivity signature as a debris ball and reported this information to their viewers during severe weather coverage (C. Fain, personal communication, 2011). Therefore, the advantage in using dual-polarization information is the increase in confidence in the detection of debris from a tornado.

Previous research on dual-polarization tornadic debris signatures (DPTDS) have focused on the use of Z_{HH} , velocity (radial or storm relative), correlation coefficient (ρ_{hv}), and differential reflectivity (Z_{DR}) to detect tornadic debris (Ryzhkov et al. 2002, Ryzhkov et al. 2005, Scharfenberg et al. 2005, Bluestein et al. 2007, Kumjian and Ryzhkov 2008, Petersen et al. 2008, Carey et al. 2008, Schultz et al. 2010, Snyder et al. 2010, Bodine et al. 2011, Carey et al. 2011, Lemon et al. 2011, Palmer et al. 2011, Schultz et al. 2011, Bodine et al. 2012, Tanamachi et al. 2012). Only three of these studies indicated that the DPTDS was used in real-time severe weather operations (Scharfenberg et al. 2005, Schultz et al. 2010, Schultz et al. 2011).

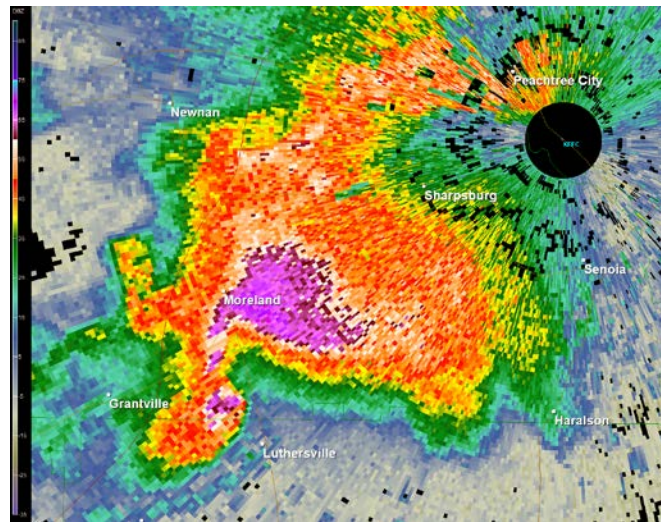


Figure 2. A tornado warned supercell with strong reflectivity that mimics a debris ball at 1954 UTC on March 26, 2011, from KFFC, near Atlanta, GA. The scale for Z_{HH} is in dBZ.

Ryzhkov et al. (2005) and Kumjian and Ryzhkov (2008) discuss the DPTDS at length at S band. They determined that DPTDSs were found within areas of high Z_{HH} (> 45 dBZ), low ρ_{hv} (< 0.80), near zero Z_{DR} , and a strong differential velocity signature in azimuth. Ryzhkov et al. (2005), Bluestein et al. (2007) and Kumjian and Ryzhkov (2008) all discussed how ρ_{hv} is the most reliable polarimetric indicator of a DPTDS as compared to Z_{DR} . Bodine et al. (2012) discusses the relationship between the DPTDS and estimation of tornado damage severity and extent in near real-time.

Similar findings for debris detection have been observed at C band. Petersen et al. (2008) and Carey et al. (2008) documented a DPTDS during a nocturnal EF-4 tornadic event using the ARMOR radar. Additional DPTDS detections at C-band have been presented in Kumjian and Ryzhkov (2008), Schultz et al. (2010), Bodine et al. (2011), Carey et al. (2011) and Palmer et al. (2011); however, each of these cases involved signatures found in strong mesocyclonic tornadoes spawn from supercell thunderstorms.

Thus, DPTDSs associated with tornadoes rated lower than EF-3 on the Enhanced Fujita Scale (EF-scale; e.g., Edwards et al. 2010) have not been well documented. Though DPTDSs have been well documented in the literature (e.g., Ryzhkov et al. 2005, Bluestein et al. 2007, Kumjian and Ryzhkov 2008, Snyder et al. 2010, Palmer et al. 2011, Kumjian 2011, Tanamachi et al. 2012), the goal of this article is to demonstrate examples of the DPTDS from a variety of convective modes at C band. Herein, examples are provided of tornadic debris signatures associated with weaker tornadoes, in a variety of convective morphologies (e.g., supercell, quasi-

linear convective system (QLCS), mesoscale convective vortex (MCV), and broken convective lines). Finally, a summary of DPTDS characteristics are presented and their implications to operational meteorology are discussed.

2. Data collection, polarimetric relation to tornadic debris, and methodology

Data was collected using UAHuntsville's ARMOR C-band dual-polarization radar located at the Huntsville International Airport (Petersen et al. 2007). ARMOR is operational 24 hours a day, 7 days a week, and has the capability for real-time sector scanning, which allows for high temporal volumetric data to be acquired when severe or hazardous weather threatens the lower Tennessee Valley. ARMOR has a 1.0° beam width and transmits at slant 45° (simultaneous H/V mode) in order to obtain measurements at both H and V polarizations. Variables that are collected using this technique are: Z_{HH} , radial velocity (V_r), Doppler spectrum width (W), Z_{DR} , ρ_{hv} (also abbreviated CC in the National Oceanic and Atmospheric Administration's Warning Decision Training Branch modules; WDTB 2011), and differential phase (Ψ_{dp}). Differential propagation phase (Φ_{dp}) is then calculated by subtracting radar system offsets, backscatter differential phase, and background noise from Ψ_{dp} . Finally, specific differential phase (K_{DP}) is determined by calculating changes in Φ_{dp} over a specific range (e.g., km^{-1}).

As stated above, the most reliable polarimetric variable for confirmation of debris is ρ_{hv} (e.g., Ryzhkov et al. 2005, Bluestein et al. 2007, Carey et al. 2008, Kumjian and Ryzhkov 2008, Petersen et al. 2008, Carey et al. 2011, Lemon et al. 2011, Schultz et al. 2011). ρ_{hv} is the correlation of the pulse to pulse returns between horizontal and vertical polarizations in a particular radar volume and is a measure of the homogeneity or heterogeneity of the scatterers in that given volume. Thus, if the volume contains hydrometeors of the same size, shape and type, then ρ_{hv} would be close to 1.0, but if a mixture of hydrometeors were present (e.g., rain and hail, or rain and snow), ρ_{hv} values would decrease below 1.0 (Balakrishnan and Zrnice 1990).

At S band values for hydrometeors are typically > 0.80 and values at or below 0.80 are likely not meteorological scatterers. Some overlap between the two types of scatterers can occur between 0.75 and 0.80 in cases of large hail and rain/hail mixtures (e.g., Straka et al. 2000, Payne et al. 2011). ρ_{hv} values greater than 0.95 at C band have been associated with rain or pure snow (e.g., Bringi et al. 1991, Carey et al. 2000, Keenan et al. 2000, Bringi and Chandrasakear 2001), while values between 0.65-0.95 at C band have been associated with hail or a mixture of hydrometeor types (e.g., Balakrishnan and Zrnice 1990, Tabary et al. 2009, Anderson et al. 2011), and can occasionally dip below 0.65 in hail (Picca and Ryzhkov 2012). Minimum ρ_{hv} values will be slightly lower for similar scatterer types (e.g., rain, rain/hail mix, Table 1) at C band as compared to S band because resonance and Mie effects occur at smaller diameters and are more pronounced at shorter wavelengths as scatterer diameter increases. However it is the variation in the backscatter that one can still take advantage of to discern debris in the radar volume, no matter the wavelength of the radar. A summary of differences between C- and S- band for rain, rain/hail mixtures and debris for ρ_{hv} have been provided in Table 1.

For tornadic debris detection, a few different thresholds on ρ_{hv} have been suggested. Ryzhkov et al. (2005) speculated that light debris (e.g., leaves and grass) likely had signatures that were approximately at 0.70 and the presence of larger debris (i.e., structural materials) depressed ρ_{hv} values even further. WDTB training on DPTDSs suggested a maximum value for ρ_{hv} of 0.80 for tornadic debris detection. WDTB also recently noted that extremely large hail can

have ρ_{hv} values in the 0.70-0.80 range at S band (e.g., Payne et al. 2011), thus some overlap does exist between hail and debris if this threshold is used. Other studies (e.g., Carey et al. 2011) reduced the maximum ρ_{hv} value for debris detection down to 0.60, but utilization of this lower threshold could miss lighter debris. The main reasons why the Carey et al. study utilized a lower threshold was to eliminate the possibility of contamination from wet melting hail that was shown to drive ρ_{hv} values toward the 0.70 threshold in C band (e.g., Tabaray et al. 2009, Anderson et al. 2011, Picca and Ryzhkov 2012) and to mitigate clutter and beam filling artifacts, especially in automated detection of debris (e.g., see Schultz et al. 2012, hereafter, Part II).

Table 1. Summary of ρ_{hv} and Z_{DR} values at S and C band for rain, rain/hail mixture and debris.

S band (10 cm)	Z_{DR} (dB)	ρ_{hv}
rain	0.5 - 8.0	0.95-1.0
rain/hail mix	≈ 0.0 - 4.5	0.75-1.0
debris	≤ 0.0	< .80
C band (5 cm)	Z_{DR} (dB)	ρ_{hv}
rain	≥ 1.0	0.93-1.0
rain/hail mix	≥ 2-3	0.65-0.95
debris	≤ 0.0	< 0.7

In addition to ρ_{hv} , Z_{DR} can also be useful for tornadic debris detection. Z_{DR} is a measure of the reflectivity-weighted oblateness of scatterers in a radar volume, and is a function of hydrometeor diameter (e.g., Seliga and Bringi 1976, Jameson 1983, Bringi and Chandrasekar 2001, p. 381). Simply put, Z_{DR} is base 10 log of the ratio of horizontal and vertical returned power. Z_{DR} has a varying array of ranges for numerous hydrometeor types at different wavelengths. Z_{DR} can also be negatively biased by differential attenuation and the overall effect is dependent upon radar wavelength and medium that the radar beam travels through.

At S-band for precipitation when Z_{HH} is large, near zero values of Z_{DR} have indicated large hail (Bringi et al. 1984, Illingworth et al. 1986, Bringi et al. 1986, Aydin et al. 1990), values between 0 dB and 2.5 dB can indicate melting hail (e.g., Leitao and Watson 1984, Aydin et al. 1986, Straka et al. 2000, Heinselman and Ryzhkov 2006, Depue et al. 2007), and for heavy rain, values are generally > 2.5 dB (Bringi and Chandrasekar 2001, p. 397). Importantly, randomly oriented scatterers (i.e., lofted debris) found within a radar volume can produce values of Z_{DR} near zero at S band (e.g., Ryzhkov et al. 2005).

At C band, the interpretation of the polarimetric hail signature using Z_{DR} is very different. Resonance effects are more pronounced because of the shorter radar wavelength. Several studies have demonstrated that large hail at C band can have Z_{DR} values > 2-3 dB, especially if the hail is water coated (e.g., Vivekanandan et al. 1990, Meischner et al. 1991, Ryzhkov and Zrnić 2007, Tabary et al. 2009, Anderson et al. 2011, Borowska et al. 2011, Picca and Ryzhkov 2012). Most importantly, one must remember when using Z_{DR} in real-time operational settings that Z_{DR} can be adversely affected by differential attenuation, resulting in negatively biased Z_{DR} values. (e.g., Bringi et al. 1990, Ryzhkov and Zrnić 1995, Smyth and Illingworth 1998, Carey et al. 2000,

Bringi et al. 2001, Tabary et al. 2009, Borowska et al. 2011). This occurrence is most prominent at shorter wavelengths.

Z_{DR} can be biased when liquid hydrometeors are present near a tornadic debris signature (i.e., > 1 dB, Ryzhkov et al. 2005), or when differential attenuation is present within the volume (e.g., Bringi et al. 1990, Vivekanandan, et al. 1990, Carey et al. 2000, Bringi et al. 2001, Gourley et al. 2007, Tabary et al. 2009, Borowska et al. 2011). Therefore, Z_{DR} should not be used in regions of large attenuation (e.g., differential propagation phase $> 30^\circ$ at S band, Smyth and Illingworth 1998, 15° at C band, Carey et al. 2000) unless the data were corrected for attenuation (e.g., Bringi et al. 1990, Vivekanandan, et al. 1990, Borowska et al. 2011). The values at S and C band for rain, rain/hail and debris for Z_{DR} have been summarized in Table 1.

In this study the following sets of rules were employed to determine DPTDS events in the ARMOR radar data. First, a strong differential velocity signature in azimuth must be present within the radar volume. Next, the rotation must be collocated with a strong return in Z_{HH} , generally greater than 30 dBZ¹. Third, ρ_{hv} values must be ≤ 0.70 ¹ and be spatially and temporally collocated with both the reflectivity and strong differential velocity signature in azimuth. In cases where heavy precipitation was near the signature and large differential attenuation was not present (i.e. $\Phi_{dp} < 15^\circ$), Z_{DR} was used for extra confidence to separate debris from rain and hail.

DPTDS heights and diameters were determined manually using the GR2Analyst software package. The center of the signature was used to obtain the height of the DPTDS. The diameter was measured by summing the number of radar range gates where the DPTDS was observed at the lowest elevation scan (0.7 degrees). Because gate spacing is constant with range from the radar, this ensures that the DPTDS diameter is not as affected by beam spreading that occurs if the diameters were to be measured between radar azimuths. Minor range effects could occur at the near and far edges of a distant DPTDS due to radar sampling. Also, when comparing DPTDS diameters, it must be emphasized to examine diameters at similar ranges; where the radar beam intersects the debris lofted by the tornado at similar heights.

Table 2. List of storm types that produced DPTDS events, the number of tornado events with observed DPTDS events, and the distribution of EF ratings with each tornado.

Type	Number	EF rating					
		EF0	EF1	EF2	EF3	EF4	EF5
Supercell	9	0	0	2	2	4	1
Broken Line	6	1	2	3	0	0	0
QLCS	3	0	3	0	0	0	0
MCV	1	0	0	1	0	0	0
Total	19	1	5	6	2	4	1

¹ WDTB criteria for S band are slightly different: $Z_H > 20$ dBZ, ρ_{hv} values < 0.80 in spatial proximity to a rotational signature are indicative of debris. Techniques and examples outlined in this article are applicable at both C and S band. More training information can be found at: <http://www.wdtb.noaa.gov/courses/dualpol/index.html>.

3. Case Examples

A total of 19 DPTDSs (128 radar volumes) are analyzed that occurred between February 6, 2008 and April 27, 2011. The tornadoes associated with the signatures were rated between EF-0 and EF-5. DPTDSs have been observed in conjunction with tornadoes spawned by supercellular thunderstorms, convective lines, a QLCS, and an MCV across North Alabama (Table 2). This section will focus on signatures seen in weaker tornadoes and culminate with an example from a strong tornado.

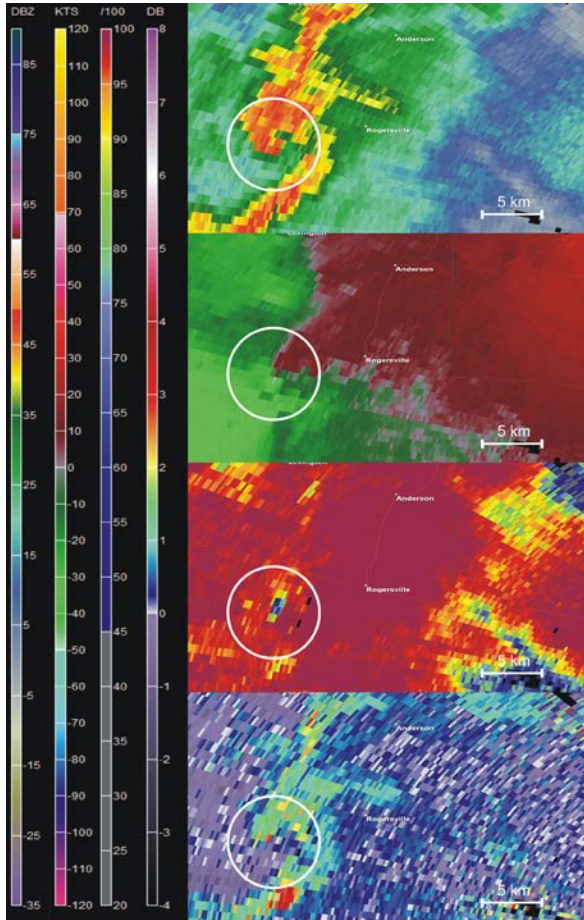


Figure 3. The DPTDS associated with the Leighton EF-2 tornado that developed out of a broken line of convection on May 8, 2008. Z_{HH} (top), V_r (upper middle), ρ_{hv} (lower middle) and Z_{DR} (bottom) are presented at 1751 UTC. Scales on the left are as follows: reflectivity (dBZ), V_r (KTS), and ρ_{hv} (value*100.0). White circles highlight the tornadic circulation, and the white length scale in the lower right corner denotes 5 km in length.

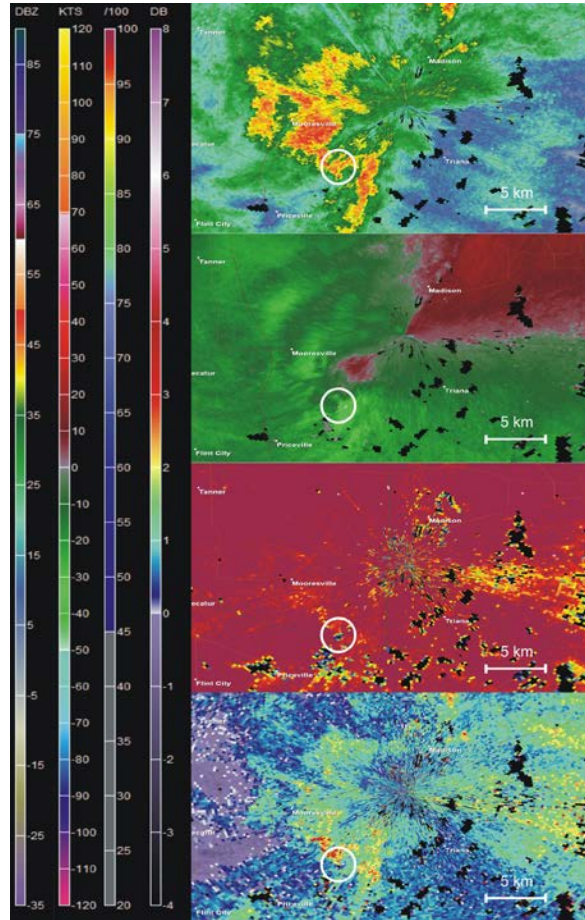


Figure 4. The DPTDS associated with the Limestone/Madison EF-1 tornado on May 8, 2008. Z_{HH} (top), V_r (upper middle), ρ_{hv} (lower middle) and Z_{DR} (bottom) are presented at 1930 UTC. Scales are the same as in Figure 3.

a. May 8, 2008, North-central Alabama

Seven tornadoes developed in the NWS Huntsville County Warning Area (CWA) out of broken portions of a linear convective system and DPTDSs were observed with three of these tornadoes. The following two examples are shown to demonstrate that debris from weaker tornadoes can be detected using dual-polarization radar. In each of these signatures notice that there is not an obvious debris ball in reflectivity, but the debris is still clearly evident in ρ_{hv} .

Figure 3 is at 1751 UTC as a tornado that originally touched down near Leighton, AL at 1739 UTC and continued to rapidly move northeastward. The tornado is wrapped in rain; however, one can still discern the clear lowering in ρ_{hv} associated with tornadic debris. A differential velocity signature in azimuth was present in Vr (differential velocity ranged from 27.0 to 39.5 m s^{-1}), ρ_{hv} values were as low as 0.50, Z_{DR} was ~ 0 dB, and the maximum diameter of the DPTDS was about 2 km. Importantly, this signature was not detected until the tornado had been on the ground for nearly 9 minutes. The lack of a signature early on was due to the range from the radar (> 65 km from the radar when tornado apparently touched down, < 60 km once the DPTDS was observed), and the strength of the tornado, as NWS storm survey information pin the strongest rating of this tornado between Leighton and Rogersville, AL, near the region that the first DPTDS was observed.

Another debris signature was observed near Huntsville's International Airport at 1930 UTC (Fig. 4). This tornado was rated EF-1 and was not immediately reported, mainly because it affected rural agricultural land and portions of the Wheeler Wildlife Reserve. A differential velocity signature in azimuth was present in Vr (differential velocity peaked at 36.0 m s^{-1} ; 27.4 m s^{-1} inbound, 8.5 m s^{-1} outbound, separated by 0.29 km), ρ_{hv} dropped as low as 0.32, Z_{DR} was slightly negative, and likely negatively biased due to differential attenuation as Φ_{dp} was approximately 20-30°. The maximum diameter of the signature was approximately 0.8 km. Here it is important to note that ρ_{hv} dipped considerably in a region where the primary debris type was biomass, thus destruction of large manmade structures is not always needed for significant lowering of ρ_{hv} within a DPTDS.

b. April 2, 2009, Tanner Crossroads tornado

On April 2, 2009, four short-lived rain-wrapped tornadoes rated EF-0 or EF-1 developed from a broken line of convection. The example shown in Figure 5 from 2136 UTC was associated with a tornado rated EF-0, estimated only to have winds of 80 mph. Despite its weak nature, the DPTDS was clearly present on radar during this tornado's 2.7 km track. This signature was present for a total of 4 minutes and associated with three 1-2 minute volume scans from ARMOR. The diameter of the DPTDS was tiny, as its maximum width was between 0.3 and 0.4 km. A differential velocity signature in azimuth was present in Vr (differential velocity ranged from 36.0 to 42.0 m s^{-1}), ρ_{hv} dipped as low as 0.58, Z_{DR} was ~ 0 dB, and there was no discernible debris ball in reflectivity. The detection of this small short-lived signature is because of the radar scanning strategy implemented and the range of the tornado from the radar (~ 20 km). This example illustrated that one can detect debris from even the weakest of tornadoes, but is greatly dependent upon the radar scanning strategy and the tornado's range from the radar.

c. April 27, 2011, morning MCV

The first of four rounds of severe convection that moved through North Alabama on this day was a convective line, with an embedded MCV. This MCV produced 16 tornadoes across Central and Northeastern AL, with several of them rated at EF-2 strength (Mullins et al. 2011). In particular, this section will focus on the initial portion of the Cold Springs-Hanceville-Holly Pond, AL, EF-2 tornado produced damage for 50 km. However, the signature associated with this tornado was only observed between 1048 and 1051 UTC as the tornado was near Cold Springs, AL. Figure 6 shows a differential velocity signature in azimuth was present in Vr (differential velocity ranged from 37.0 to 49.1 m s⁻¹) and was coupled with low ρ_{hv} values (0.56-0.66), moderate reflectivity (30-40 dBZ) and $Z_{DR} \leq 0$ dB. In this case Z_{DR} is negatively biased due to differential attenuation from heavy precipitation (Φ_{dp} was $\sim 105^\circ$); therefore, Z_{DR} is underestimated but still highlights a relative minimum within the DPTDS. Importantly, ρ_{hv} clearly indicates that tornadic debris was present in this situation.

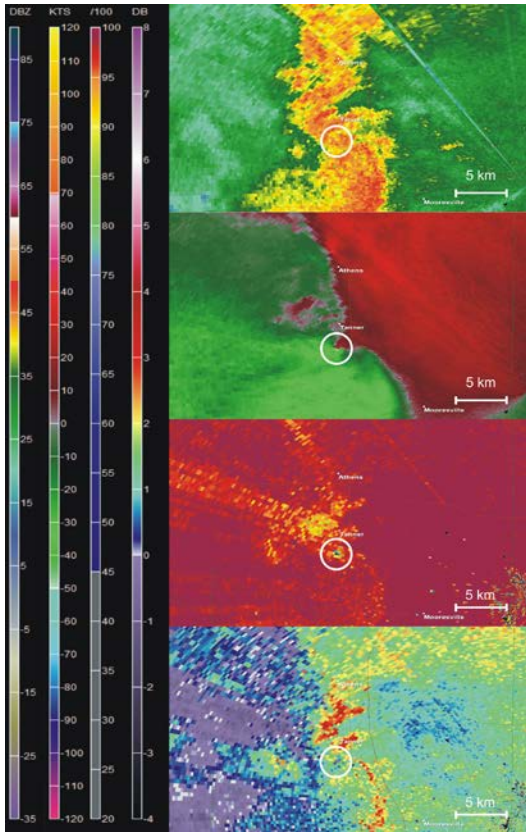


Figure 5. The DPTDS associated with the Tanner Crossroads EF-0 tornado that developed out of a line of convection on April 2, 2009. Z_{HH} (top), V_r (upper middle), ρ_{hv} (lower middle) and Z_{DR} (bottom) are presented at 2136 UTC. Scales are the same as in Figure 3.

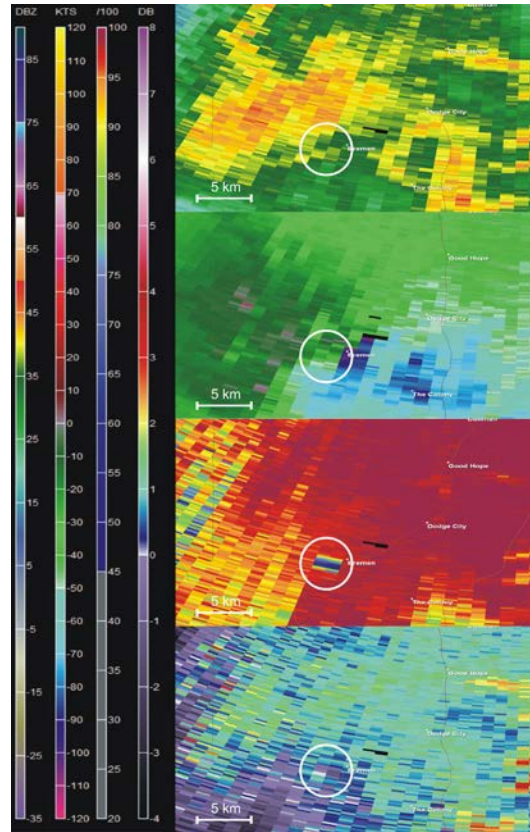


Figure 6. The DPTDS associated with the beginning of the morning Cold Springs/Hanceville/Holly Pond, AL EF-2 tornado from April 27, 2011. Z_{HH} (top), V_r (upper middle), ρ_{hv} (lower middle) and Z_{DR} (bottom) are presented at 1049 UTC. Scales are the same as in Figure 3.

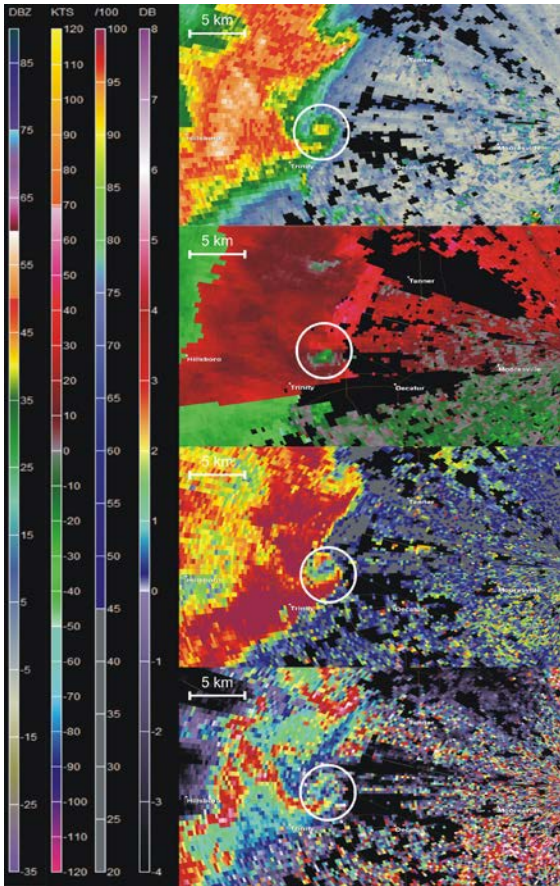


Figure 7. ARMOR radar images from 2026 UTC on April 27, 2011 of the DPTDS associated with the Hackleburg EF-5 tornado in Z_{HH} (top), V_r (upper middle), ρ_{hv} (lower middle) and Z_{DR} (bottom). Scales are the same as in Figure 3.

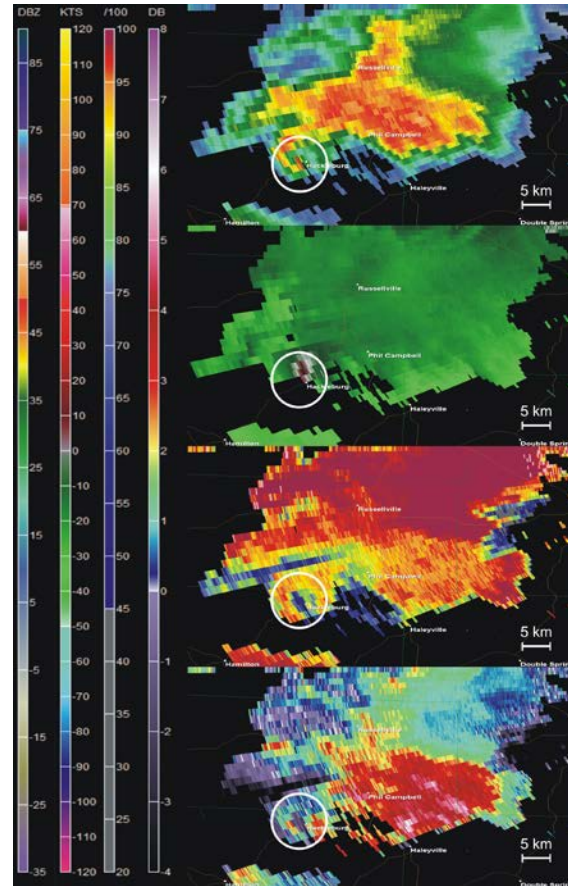


Figure 8. ARMOR radar images from 2026 UTC on April 27, 2011 of the DPTDS associated with the Hackleburg EF-5 tornado in Z_{HH} (top), V_r (upper middle), ρ_{hv} (lower middle) and Z_{DR} (bottom). Scales are the same as in Figure 3.

d. April 27, 2011, midday QLCS

QLCS tornadoes are often harder to detect and not as long lived as some of their supercell counterparts. However, in spite of their relative brevity, debris from these tornadoes can be detected like any other tornado. One example is presented below from the midday QLCS that produced 7 tornadoes in North Central AL on April 27 (Wade et al. 2011).

The example in Figure 7 is of one QLCS tornado near the Decatur Industrial Park in Decatur, AL, at 1622 UTC. There is a noticeable curl in reflectivity in conjunction with a differential velocity signature in V_r (differential velocity was 31 m s^{-1} ; 10.5 m s^{-1} inbound 20.5 m s^{-1} outbound) and lowering in ρ_{hv} . Minimum ρ_{hv} values within this signature were between 0.60 and 0.64 and Z_{DR} was $\sim 0 \text{ dB}$ during the 4 minutes that this signature was present on radar. A site survey revealed that most of this tornado's damage was trees and roofing material from several businesses within the industrial park. Furthermore, the use of the

DPTDS signature in the storm survey helped separate this EF-1 track from the EF-4 Hackleburg-Tanner-Harvest tornado that produced damage less than 1 km from this tornado track.

e. April 27, 2011, afternoon supercells

The afternoon round of severe convection brought about multiple supercells which produced 6 EF-4+ rated tornadoes within 125 km of ARMOR in North Alabama. Unfortunately, dual-polarization information from ARMOR was only collected on 5 of the 6 large tornadoes because power had been cut to the region by the time the Rainsville, AL, EF-5 tornado developed. The afternoon event yielded a total of 7 DPTDSs at a variety of ranges, many of which persisted for several tens of minutes, and were used in real-time operations by NWS Huntsville.

The most notable debris signature was observed from the Hackleburg-Tanner-Harvest, AL, EF-5 tornado. This DPTDS was seen on radar for over an hour and a half, and was at least 2 km in diameter for much of the tornado's lifetime. The first evidence of this signature was observed at a distance of 106 km as the tornado entered Hackleburg, AL (Figure 8). Due to the large number of tornadic supercell storms affecting North Alabama on this day, vertical information beyond 2.0 degrees elevation was not collected in order to provide 1-minute low-level updates on multiple storms for UAHuntsville's media partner WHNT-TV, and the NWS Huntsville. Thus, the authors were only able to discern debris up to 4 km because of the low-level scanning strategy implemented during this period. Importantly, the NWS Huntsville office used the DPTDS information to aid in the warning process, especially during long periods of time when reports of the tornado were not being received by the office.

4. Additional characteristics of the DPTDS

This next section explores the overall characteristics of the DPTDS from all 19 events collected in North Alabama. 128 unique radar volumes were analyzed to determine any trends that may be present in this study's small sample of cases. Also, examined in detail is the Cullman DPTDS to demonstrate temporal changes in characteristics of the DPTDS during a long track tornado. In the following section EF-ratings are utilized as a measure of strength for each DPTDS event at various ranges from the radar.

Comparing diameters at similar ranges shows that there is a slight increase of DPTDS diameter associated with stronger tornadoes (Fig. 9). However, at several ranges weak events and stronger event diameters overlap. This overlap is most notable at 5 km, 30 km, and 60 km from the radar. Similarly, some of the highest heights that debris is lofted within this sample occur with the strongest tornadoes (EF2+; Fig. 10). The highest observed height of debris was ~7 km (Fig. 11) in the Cullman EF-4 tornado during its peak intensity.

Thus, definitive relationships between DPTDS characteristics and EF-rating are not possible due to disconnect between what is being destroyed at the surface and how the signature appears in the radar volume. This disconnect occurs because it is difficult to determine exactly what debris from the surface is within the radar volume at any given time, how long the debris has resided within the radar volume, or if the damage observed at the surface even makes it to the height which it could be observed by the radar. This is best represented by the scatter of EF-ratings found within Figs. 9 and 10. In both figures there is overlap between weak, strong

and violent tornadoes for both diameter and height. Because the final tornado strength rating is not based upon radar characteristics of the tornado; relationships between DPTDS characteristics and current ways of measuring tornado damage strength are difficult because damage observed at the surface does not always correspond to the size and height characteristics of the signature.

5. Discussion

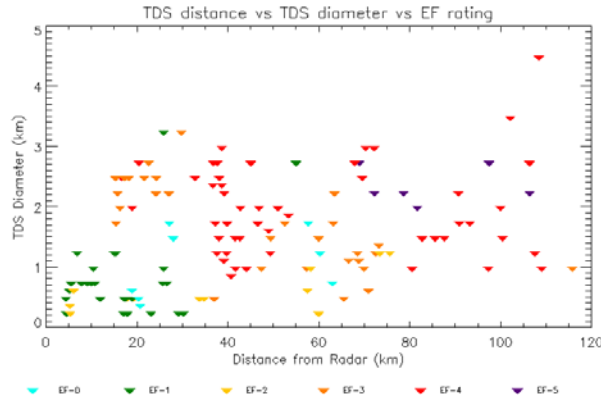


Figure 9. Presented is a compilation of all 19 DPTDS examining distance from radar versus diameter of the DPTDS signature. EF- ratings are provided for the reader's value to understand the estimated strength of the tornado at the surface. Comparisons between diameters should be made at similar distances from the radar to ensure that the radar beam is intersecting the lofted debris from the tornado at a similar height.

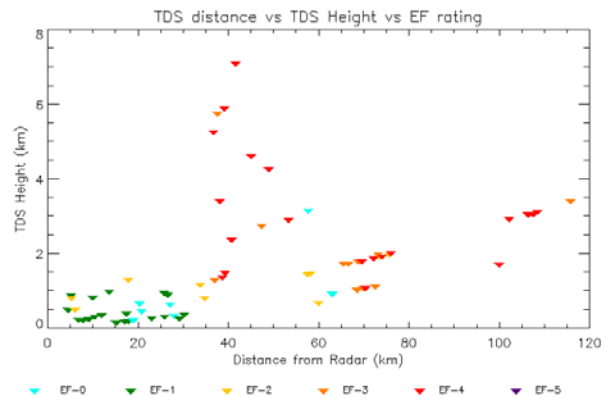


Figure 10. Presented is a compilation of all 19 DPTDS events where the maximum height of the signature is known, examining distance from the radar and the height of the DPTDS. EF- ratings are provided for the reader's value to understand the estimated strength of the tornado at the surface.

There are several operational implications to the observance of DPTDS events. First, these signatures can be used as storm spotter reports if used correctly. There have been several instances where there is a lack of reporting while large violent tornadoes are producing their most significant damage (e.g., Glass 2011). Sometimes spotter reports are delayed by several minutes (e.g., Witt et al. 1998, Williams et al 1999) because of the severity of the damage. During the April 27, 2011 outbreak there were several periods of time where there was a distinct lack of reporting on strong tornadoes due to significant damage. For instance, while the Hackleburg-Tanner-Harvest EF-5 tornado was producing significant damage in rural Lawrence Co. AL, there was an 18 minute period where zero reports of the tornado were received by the NWS Huntsville (Iowa Environmental Mesonet, 2011). Radar based indications from KHTX and the WSR-88D radar at Columbus AFB, MS, indicated that tornado was likely present, so the ARMOR information provided confirmation during this period of time without reports. Furthermore, as shown in Schultz et al. (2010), the DPTDS could be used to confirm storm spotter reports. This can be useful during night time, complex terrain, and rain-wrapped tornado events where visibility might be limited or hindered, as has been outlined in other studies. While the DPTDS cannot pinpoint exact locations of the ground path given displacement between the ground location and the radar observed location of the tornado, it can provide general areas to search for a damage path or help separate two paths that may be in close proximity to each other.

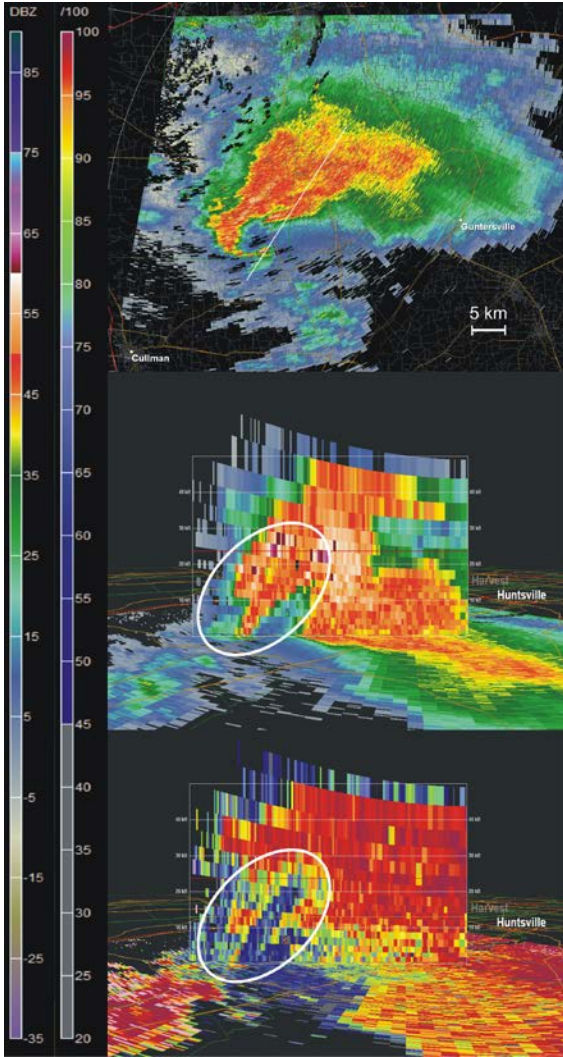


Figure 11. ARMOR radar images from 2016 UTC on April 27, 2011. ZHH (top, middle), ρ_{hv} (bottom). The middle and bottom panels are vertical cross sections through the storm and the cross section is taken along the white line in the top panel. Scales on the left are as follows: reflectivity (dBZ), and ρ_{hv} (value*100.0). 10,000 ft is approximately 3 km. Volume time is 146s.

scanning strategy implemented. Also, there can be a lag in tornado touchdown time and debris manifestation in the radar volume. This point is further addressed in Part II. It must be stressed that standard procedures for identifying tornadic circulations must be followed first before searching ρ_{hv} for debris. This point has been made both in WDTB training and Lemon et al. (2011), and lowers the possibility of false detection of debris.

As indicated in the previous section definitive relationships between EF- strength and DPTDS characteristics are currently not possible. Here we pose two simple questions. What if a violent tornado never left a region that lacked damage indicators that would bring the tornado up to a violent rating? What if the initial damage indicators during the survey result in an incorrect initial damage assessment and the rating in the forested region could be assessed higher based on information unavailable in the EF-scale guidance? Both of these issues are addressed in part by Edwards et al. (2010) and are important considerations in relating any radar derived product to current measure of tornado strength. Also, because of a lack of detailed information on surface characteristics (i.e., what is being destroyed) and how the lofted debris appears in the radar data (i.e., shape, size, orientation, dielectric, wet, dry); building relationships between the current measure of tornado strength and radar information will be difficult. This area of research will need to be studied in more detail in order to understand the various complexities of debris and debris lofting within the turbulent environment of the tornado. The DPTDS characteristics are still useful in real-time (also see Bodine et al. 2012), but will need to be used with caution when trying to make estimates in real-time as to the potential strength or longevity of the tornado using current methods for rating tornadoes given that there is some uncertainty in the relationship between the DPTDS characteristics and observed damage at the surface as seen in Figs. 9 and 10.

Finally, not every tornado that occurs within the viewing range of dual-polarization radar produced a DPTDS. Limitations include range of the tornado from the radar and radar

6. Conclusions

Multiple examples of DPTDS events have been presented from a variety of tornado producing storm types using the ARMOR C-band radar. As suggested by several previous works, ρ_{hv} was the most reliable polarimetric variable in detection of tornadic debris. DPTDS events were detected for both weak ($<EF2$) and strong to violent ($\geq EF2$) tornado events. Some DPTDS events appeared on short time scales which may prove difficult for current WSR-88D scan strategies. Another useful application of the DPTDS is during the post event storm surveys, as shown in Case Examples, Sections 3a. and 3d. There is a slight indication that DPTDS diameters were larger for the stronger tornadoes, and that debris from stronger tornadoes were seen at far distances and high altitudes. However, these events indicate no definitive relationships between current methods of rating tornadoes and DPTDS characteristics. Currently it is difficult to form an EF-rating from radar information alone due to the lack of information on surface characteristics (what is being destroyed) and shape, size, dielectric and orientation within the radar volume of the various scatterers lofted by the tornado.

Potential does exist in using the DPTDS for general estimation of tornado characteristics in near real-time (e.g., weak/strong short/long-lived) in some of the events presented here based on Figs. 9 and 10 and in Bodine et al. (2012). However there also will be times when these relationships break down, which is why only an official NWS ground survey can provide the final EF-rating for a tornado. Future work examining the feasibility of using the DTPDS in real-time on a larger sample of cases should include the probability and uncertainty that exists in real-time estimation of tornado strength. This work should also include examples from the operational forecasting community to determine if polarimetric tornado estimation can be accomplished during severe weather episodes. Also, it will be important to perform empirical and modeling studies to show various types of debris appear in the radar volume. This type of work would confirm the thresholds currently employed for debris detection, and would provide insight to what types of debris may be within a radar volume at a given time. Additional examples and caveats from operational experience are presented in Part II, and will provide the reader with useful information for operational applications.

Acknowledgements. The authors would like to thank Paul Schlatter for valuable discussions on debris signatures that have been observed with the new WSR-88D S-band dual-polarization data, as well as providing insight into the training modules of WDTB. Suheily López Belén's excellent contour maps were of great help when associating radar information to ground damage rating. A final thank you goes out to all of the National Weather Service staff (both locally and from other portions of the country), NASA SPoRT, and UAHuntsville students who have spent tireless hours meticulously rating and mapping tornado damage paths, specifically after the April 27, 2011 tornado outbreak. Without their hard work, much of this study would not be possible, as detailed ground survey information would have not been collected. UAHuntsville co-authors wish to acknowledge support from NOAA Grant NA090AR4600204. C. Schultz would like to acknowledge additional support through the NASA Cooperative Education Program at NASA Marshall Space Flight Center. The authors would like to thank the two anonymous reviewers for their constructive and critical reviews, which greatly aided in the development of this article.

REFERENCES

- Anderson, M. E., L. D. Carey, W. A. Petersen, and K. R. Knupp, 2011: C-band dual-polarimetric radar signatures of hail. *Electronic J. Operational Meteor.*, **12** (2), 45-75.
- Aydin, K., Zhao, Y., and Seliga, T. A., 1990: A differential reflectivity radar hail measurement technique: Observations during the Denver hailstorm of 13 June 1984. *J. Atmos. and Oceanic Tech.*, **7**, 104-113.
- , T. Seliga, and V. Balaji, 1986: Remote sensing of hail with dual linear polarization radar. *J. Climate Appl. Meteor.*, **25**, 1475-1484.
- Balakrishnan N., and D. S. Zrnic, 1990: Use of polarization to characterize precipitation and discriminate large hail. *J. Atmos. Sci.*, **47**, 1525-1540.
- Bluestein, H. B., M. M. French, R. L. Tanamachi, S. Frasier, K. Hardwick, F. Junyent, and A. L. Pazmany, 2007: Close-range observations of tornadoes in supercells made with a dual-polarization, X-band, mobile Doppler radar. *Mon. Wea. Rev.*, **135**, 1522–1543. doi: 10.1175/MWR3349.1
- Bodine, D. J., M. R. Kumjian, R. D. Palmer, P. L. Heinselman, and A. V. Ryzhkov, 2012: Tornado damage estimation using polarimetric radar. *Wea. and Forecasting*, in press. doi: 10.1175/WAF-D-11-00158.1
- Bodine, D., M. R. Kumjian, A. J. Smith, R. D. Palmer, A. V. Ryzhkov, and P. L. Heinselman, 2011: High resolution polarimetric observations of an EF-4 tornado on 10 May 2010 from OU-PRIME. *35th Conf. on Radar Meteorology*, Pittsburgh, PA, Amer. Met Soc.
- Borowska, L., A. Ryzhkov, D. Zrnić, C. Simmer, and R. Palmer, 2011: Attenuation and differential attenuation of 5-cm-wavelength radiation in melting hail. *J. Appl. Meteor. Climatol.*, **50**, 59–76. doi: 10.1175/2010JAMC2465.1
- Bringi, V. N., and V. Chandrasekar, 2001: *Polarimetric Doppler Weather Radar: Principles and Applications*. Cambridge University Press, Cambridge, 636 pp.
- , T. A. Seliga, and K. Aydin, 1984: Hail detection with a differential reflectivity radar. *Science*, **225**, 1145-1147.
- , J. Vivekanandan, and J. D. Tuttle, 1986: Multiparameter radar measurements in Colorado convective storms. Part II: Hail detection studies. *J. Atmos. Sci.*, **43**, 2564-2577.
- , V. Chandrasekar, N. Balakrishnan, and D. S. Zrnić, 1990: An examination of propagation effects in rainfall on radar measurements at microwave frequencies. *J. Atmos. Oceanic Technol.*, **7**, 829–840.
doi:10.1175/1520-0426(1990)007<0829:AEOPEI>2.0.CO;2

- , V. Chandrasekar, P. Meischner, J. Hubbert, and Y. Golestani, 1991: Polarimetric radar signatures of precipitation at S- and C-bands. *IEEE Trans. Remote Sens.*, **138**, 109-119.
- , G.-J. Huang, V. Chandrasekar, and T. D. Keenan, 2001: An areal rainfall estimator using differential propagation phase: Evaluation using a C-band radar and a dense gauge network in the tropics. *J. Tech.* **18**, 1810–1818.
- Bunkers, M. J., and M. A. Baxter, 2011: Radar tornadic debris signatures on 27 April 2011. *EJOM*, **ION-1**.
- Carey, L. D., S. A. Rutledge, D. A. Ahijevych, and T. D. Keenan, 2000: Correcting propagation effects in C-band polarimetric radar observations of tropical convection using differential propagation phase. *J. Appl. Meteor.*, **39**, 1405-1433.
- , W. A. Petersen, and K. R. Knupp, 2008: ARMOR dual-polarimetric radar observations of two tornadic supercells during the 2008 Super-Tuesday tornado outbreak. *33rd NWA Annual Meeting*, Louisville, KY, Natl. Wea. Assoc.
- , C. J. Schultz, E. V. Schultz, W. A. Petersen, P. N. Gatlin, Kevin R. Knupp, A. L. Molthan, G. J. Jedlovec, and C.B. Darden, 2011: Dual-polarimetric radar-based tornado debris paths associated with EF-4 and EF-5 tornadoes over northern Alabama during the historic outbreak of 27 April 2011. *36th Annual NWA Conference*, Birmingham, AL, Natl. Wea. Assoc.
- Crum, T. D., and R. L. Alberty, 1993: The WSR-88D and the WSR-88D operational support facility. *Bull. Amer. Meteor. Soc.*, **74**, 1669–1687. doi: 10.1175/1520-0477(1993)074<1669:TWATWO>2.0.CO;2
- Depue, T. K., P. C. Kennedy, and S. A. Rutledge, 2007: Performance of the hail differential reflectivity (HDR) polarimetric radar hail indicator. *J. Appl. Meteor. Clim.*, **46**, 1290-1301.
- Edwards, R. E., J. G. LaDue, J. T. Ferree, K. A. Scharfenberg, C. Maier, and W. L. Coulbourne, 2010: The Enhanced Fujita Scale: Past, present and future. *25th Conf. on Severe Local Storms*, Denver, CO, Amer. Met. Soc. [Available online at <https://ams.confex.com/ams/25SLS/webprogram/Paper175400.html>]
- Forbes, G., 2011: Terrible 2011 tornadoes. *36th Annual NWA Conference*, Birmingham, AL, Natl. Wea. Assoc.
- Glass, F., 2011: Warning operations and decision making for the St. Louis tornadoes on Good Friday, 22 April 2011. *36th Annual NWA Conference*, Birmingham, AL, Natl. Wea. Assoc.

- Gourley, J. J., P. Tabary, and J. Parent du Chatelet, 2007: Empirical estimation of attenuation from differential propagation phase measurements at C-band. *J. Appl. Meteor. Climatol.*, **46**, 306–317. doi: 10.1175/JAM2464.1
- Heinselman, P. L., and A. V. Ryzhkov, 2006: Validation of polarimetric hail detection. *Wea. Forecasting*, **21**, 839-850.
- Illingworth, A. J., J. W. F. Goddard, and S. M. Cherry, 1986: Detection of hail by dual polarization radar. *Nature*, **320**, 431-433.
- Iowa Environmental Mesonet, 2011: IEM Cow. <http://mesonet.agron.iastate.edu/cow/>
- Jameson, A. R., 1983: Microphysical interpretation of multi-parameter radar measurements in rain. Part I: Interpretation of polarization measurements and estimation of raindrop shapes. *J. Atmos. Sci.*, **40**, 1792–1802. doi: 10.1175/1520-0469(1983)040<1792:MIOMPR>2.0.CO;2
- Keenan, T. D., L. D. Carey, D. S. Zrnić, and P. T. May, 2000: Sensitivity of 5-cm wavelength polarimetric radar variables to raindrop axial ratio and drop size distribution. *J. Appl. Meteor.*, **40**, 526-545.
- Kumjian, M. R., 2011: Precipitation properties of supercell hook echoes. *Electronic J. Severe Storms Meteor.*, **6** (5), 1–21.
- , and A. V. Ryzhkov, 2008: Polarimetric signatures in supercell thunderstorms. *J. Appl. Meteor. Climatol.*, **47**, 1940–1961. doi: 10.1175/2007JAMC1874.1
- Lemon, L. R., C. A. Van Den Broeke, C. Payne, and P. T. Schlatter, 2011: Dual polarimetric Doppler radar debris signature characteristics of a long-track EF-5 tornado. *36th Annual NWA Conference*, Birmingham, AL, Natl. Wea. Assoc.
- Leitao, M. J., and P. A. Watson, 1984: Application of dual linearly polarized radar data to prediction of microwave path attenuation at 10-30 GHz. *Radio Sci.*, **19**, 209-221.
- Meischner P. F., V. N. Bringi, D. Heimann, and H. Holler, 1991: A squall line in southern Germany: Kinematics and precipitation formation as deduced by advanced polarimetric and Doppler radar measurements. *Mon. Wea. Rev.*, **119**, 678-701.
- Mullins, S., and K. R. Knupp, 2011: Analysis of the North Alabama MCV on the morning of 27 April 2011. *36th Annual NWA Conference*, Birmingham, AL, Natl. Wea. Assoc.
- Palmer, R. D., and Coauthors, 2011: Observations of the 10 May 2010 tornado outbreak using OU-PRIME: Potential for new science with high-resolution polarimetric radar. *Bull. Amer. Meteor. Soc.*, **92**, 871–891. doi: <http://dx.doi.org/10.1175/2011BAMS3125.1>

- Payne, C., and L. R. Lemon, 2011: Identifying significant severe-size hail with S-band dual polarization radar. *36th Annual NWA Conference*, Birmingham, AL, Natl. Wea. Assoc.
- Picca, J., and A. Ryzhkov, 2012: A dual-wavelength polarimetric analysis of the 16 May 2010 Oklahoma City extreme hailstorm. *Mon. Wea. Rev.*, **140**, 1385–1403.
- Petersen, W. A., K. R. Knupp, D. J. Cecil, and J. R. Mecikalski, 2007: The University of Alabama Huntsville THOR Center instrumentation: Research and operational collaboration. *33rd International Conference on Radar Meteorology*, Cairns, Australia, Amer. Met. Soc.
- , L. D. Carey, K. R. Knupp, C. J. Schultz, and E. V. Johnson, 2008: ARMOR dual-polarimetric radar observations of tornadic debris signatures. *24th Conf. on Severe Local Storms*, Savannah, GA, Amer. Met. Soc.
- Ryzhkov, A., and D. S. Zrnić, 1995: Precipitation and attenuation measurements at a 10-cm wavelength. *J. Appl. Meteor.*, **34**, 2121–2134.
- , and D. S. Zrnić, 2007: Depolarization in ice crystals and its effect on radar polarimetric measurements. *J. Atmos. Oceanic Technol.*, **24**, 1256–1267.
- , D. W. Burgess, D. S. Zrnić, T. Smith, and S. E. Giangrande, 2002: Polarimetric analysis of a 3 May 1999 tornado. Preprints, *21st Conf. on Severe Local Storms*, San Antonio, TX, Amer. Meteor. Soc., 515–518.
- , T. J. Schuur, D. W. Burgess, and D. S. Zrnić, 2005: Polarimetric tornado detection. *J. Appl. Meteor.*, **44**, 557–570. doi: 10.1175/JAM2235.1
- Scharfenberg, K. A., and Coauthors, 2005: The Joint Polarization Experiment: Polarimetric radar in forecasting and warning decision making. *Wea. Forecasting*, **20**, 775–788. doi: 10.1175/WAF881.1
- Schultz, C.J., E. V. Schultz, L. D. Carey, W. A. Petersen, B. C. Carcione, C. B. Darden, and D. Satterfield, 2010: The use of a dual polarimetric debris signature in the real-time operational warning environment during the April 24, 2010 tornado event in North Alabama. *NWA Newsletter*, May 2010.
- , and Coauthors 2012: Dual-polarization tornadic debris signatures Part II: Comparisons and caveats. *Electronic J. Operational Meteor.*, **13** (9) 138-150.
- , and Coauthors, 2011: The use of dual polarimetric tornadic debris signatures in an operational setting. *36th Annual NWA Conference*, Birmingham, AL, Natl. Wea. Assoc.
- Seliga, T. A., and V. N. Bringi, 1976: Potential use of radar differential reflectivity measurements at orthogonal polarizations for measuring precipitation. *J. Appl. Meteor.*, **15**, 69–76. doi: 10.1175/1520-0450(1976)015<0069:PUORDR>2.0.CO;2

- Smyth, T. J., and A. J. Illingworth, 1998: Correction for attenuation of radar reflectivity using polarization data. *Quart. J. Roy. Meteor. Soc.*, **124**, 2393-2415.
- Snyder, J. C., H. B. Bluestein, G. Zhang, and S. J. Frasier, 2010: Attenuation correction and hydrometeor classification of high-resolution, X-band, dual-polarized mobile radar measurements in severe convective storms. *J. Atmos. Oceanic Technol.*, **27**, 1979–2001. doi: <http://dx.doi.org/10.1175/2010JTECHA1356.1>
- Straka, J. M., and D. S. Zrnić, A. V. Ryzhkov, 2000: Bulk hydrometeor classification and quantification using polarimetric radar data: Synthesis of relations. *J. Appl. Meteor.*, **39**, 1341–1372.
- Tabary, P., F. Vulpiani, J. J. Gourley, A. J. Illingworth, R. J. Thompson, and O. Bousquet, 2009: Unusually high differential attenuation at C-band: Results from a two-year analysis of the French Trappes polarimetric radar data. *J. Appl. Meteor. Clim.*, **48**, 2037-2053.
- Tanamachi, R. L., H. B. Bluestein, J. B. Houser, S. J. Fraiser, and K. M. Hardwick, 2012: Mobile, X-band polarimetric Doppler radar observations of the 4 May 2007 Greensburg, Kansas tornadic supercell. *Mon. Wea. Rev.*, in press.
- Van Den Broeke, M. S., J. M. Straka, and E. N. Rasmussen, 2008: Polarimetric radar observations at low levels during tornado life cycles in a small sample of classic Southern Plains supercells. *J. Appl. Meteor. Climatol.*, **47**, 1232–1247. doi: [10.1175/2007JAMC1714.1](http://dx.doi.org/10.1175/2007JAMC1714.1)
- Vivekanandan, J., V. N. Bringi, and R. Raghavan, 1990: Multiparameter radar modeling and observations of melting ice. *J. Atmos. Sci.*, **47**, 549–564. doi: [10.1175/1520-0469\(1990\)047<0549:MRMAOO>2.0.CO;2](http://dx.doi.org/10.1175/1520-0469(1990)047<0549:MRMAOO>2.0.CO;2)
- Wade, R. A., T. A. Murphy, and K. R. Knupp, 2011: Preliminary observations of the mid-day 27 April 2011 North Alabama tornadic QLCS from multiple radar platforms. *36th Annual NWA Conference*, Birmingham, AL, Natl. Wea. Assoc.
- Warning Decision Training Branch, 2011: Dual-pol Training. [<http://www.wdtb.noaa.gov/courses/dualpol/index.html>]
- Williams, E. R., and Coauthors, 1999: The behavior of total lightning activity in severe Florida thunderstorms. *Atmos. Res.*, **51**, 245–265.
- Witt, A., M. D. Eilts, G. J. Stumpf, E. D. W. Mitchell, J. T. Johnson, and K. W. Thomas, 1998: Evaluating the performance of WSR-88D severe storm detection algorithms. *Wea. Forecasting*, **13**, 513–518.